Hierarchy in zeolite catalysis: The influence of enhanced mesoporosity on the synthesis of renewable fuels and bio-based platform chemicals

محفزات الزيولات النانوية : تاثير زيادة الطبقات السطحية على انتاج الوقود الحيوي والمواد الكيمياوية الاساسية

Aqeel Al-Ani[1,2*]; Catia Freitas[1] and Vladimir Zholobenko[1]

[1]School of Chemical and Physical Sciences, Keele University, Keele, Staffordshire, ST5 5BG, United Kingdom

[1]Ministry of Oil, Oil Marketing Company (SOMO), Baghdad, Iraq

[*]Corresponding Author E-mail: dr.aqeel.alani@gmail.com

Abstract

Faujasite (FAU), ZSM-5 (MFI), beta (BEA) and mordenite (MOR) zeolites were admitted to a variety of chemical treatments accompanied by surfactant templating strategy, aiming to introduce the intracrystalline mesoporosity effectively. The resulting materials were tested as solid acid catalysts for esterification of the oleic acid as a common model impurities found in bio-oil feedstoks. It was found that the esterification of oleic acid can be enhanced by the presence of strong acid sites in zeolites and their improved accessibility. Overall, mesostructured FAU zeolite demonstrated an improved catalytic performance as a result of increasing accessibility of the zeolite active sites.

Keywords: Esterification, Surfactant, Acid site, Accessibility, Oleic acid, Faujasite.

1. Introduction

In the last years, significant attention has been focused on sustainable and green energy applications due to oils price fluctions, environment change and cost of high quality fuels.[1, 2]

To date, the main components being used, as renewable hydrocarbon sources are triglycerides (TGs) and lignocellulose.[3, 4] However, technology for production of biofuels and chemicals has been challenged by manufacturing cost, feedstock type (edible or non-edible) and catalytic reactions.[5] The esterification reaction takes place between the free fatty acid (FFA), which present in a mixture with TGs in plant, algal and oil feedstoks with small alcohol molecule in the presence of an acid or base catalyst in order to form fatty acid methyl esters (FAME). Usually, this reaction is appropriate for feedstock containing over ~ 4% of FFA, the mixture then is converted to biodiesel via transesterification reaction using basic catalyst.[1, 6] This reaction also, is essential, especially in cheap feedstock , because the amount of free fatty acids can inhibit the activity of the basic catalyst. Although a considerable research has been undertaken utilising recoverable and non-corrosive materials such as zeolites, metal oxides, metal-organic frameworks, and metal-substituted zeotypes in these reactions,[7-25] many of these studies are not obtained high product selectivity because of mass transport limitations of small internal surface of the pores in zeolites.[26-28] At the same time, previous attempts to prepare mesoporous MCM-41and SBA-15 type materials have been overcome some of obstacles associated with zeolites. However, these materials exhibited mild acidity, lack of hydrothermal stability and low crystallinity.[26] promptly, another often observed in the field of the synthesis of well-defined architectures zeolites has been developed in 2000, which is called bottom-up and top-down approaches.[26, 29-36] Among them, the surfactant-templated zeolite mesostructuring approach has been commercialised successfully and employed in biomass processing and bio-oil upgrading.[37-40] At this point, the long-chain alkyl quaternary amine cationic surfactant mixed with zeolites in basic solution in order to produce larger pores, which can be expected to reduce the diffusion limitations toward larger molecules in the reaction mechanisum.[38]

It is now well established that from our previous work [41], the transesterification of TGs over hierarchical faujasites possessing intracrystalline networks of mesopores, the zeolite composition, and hence, the strength of basic sites has a greater impact on the activity of the catalyst than their accessibility. Moreover, in our recent work [42], the surfactant-templating mesostructuring approach has been utilised for the preparation of a number of large-pore zeolites. The catalyst preparation involves a post-synthesis modification using surfactant in

basic media, which results in the formation of a network of ordered mesopores within the zeolite .The present paper is focused on these nanostructured catalysts and on the effect of their properties on the catalytic efficiency in esterification of oleic acid as potential bio-refinery related applications.

2. Experimental section

2.1 Synthesis of hierarchical zeolites

A detailed description for preparation of these zeolites is available in Ref [42].

Faujasite zeolite (CBV100) with Si:Al molar ratio 2.5 was purchased from Zeolyst International and modified to obtain the hierarchical zeolite (HFAU2.5).The Na-type FAU zeolite was treated with 6 mol L^{-1} of ammonium nitrate solution (Sigma-Aldrich, >99 wt%) at 80°C, followed by filtering and washing , and then calcined at 450°C for 5h in static air to convert the ammonium form to H-type FAU zeolite.

The MOR (CBV 21A) and BEA (CP814C) zeolites with Si:Al molar ratio 10 and 19 respectively, were also acquired from Zeolyst International. 2 g of parent MOR and BEA zeolites were calcined in air at 450°C for 5h and then stirred in 50 mL of basic solution of 0.15-0.5 mol L^{-1} Tetramethylammonium hydroxide pentahydrate (Alfa Aesar, 98%). After that 1-1.75 g of n-cetyltrimethylammonium bromide (CTAB, Alfa Aesar, 98%) was added for this mixture. Next, after 1h, the synthesis mixtures were placed into Teflon-lined autoclaves and heated to 150°C using CEM Mars 6 microwave (CEM Corporation) at 2.45 GH. The heating time was varied from 15 h to 18 h. The initial ramp time was 20 minute and the power output did not exceed 400 W. The products were filtered and washed with deionized water.

The parent MFI (CBV 8014) zeolite with Si:Al molar ratio 40, was obtained from Zeolyst International and stirred for 30 min. at 80°C with 50 mL of basic solution containing 0.2 mol L^{-1} from Sodium hydroxide (Fisher Scientific ,98%) and tetrapropylammonium hydroxide (TPAOH,Alfa Aesar,1M) .This suspension was added to solution containing 1 g of CTAB and leave it for stirring 1h. The resulting synthesis mixture was conducted under microwave hydrothermal synthesis according to the method mentioned above for 8h to 16h.

Finally, all above solids were dried at 60°C overnight and then were calcined first in the flow of nitrogen at 450°C (temperature ramp of 1.5^{o}C min^{-1}) for 1h. Then, the gas flow was switched to oxygen, the temperature was increased to 500°C (temperature ramp of 2°C min^{-1}) and kept for 2h before cooling these samples.

2.2 Characterisation of zeolites catalysts

A comprehensive structural characterisation of all the materials utilised in this work was carried out using powder X-ray diffraction (XRD), transmission electron microscopy (TEM), low temperature nitrogen adsorption, N_2 Physisorption (BET) and FTIR spectroscopy. A detailed description is also available in Ref [42].

All the solid materials were characterized by different techniques. Powder X-ray diffraction (XRD) patterns of various catalysts were recorded on Brucker D8 Advance diffractometer with CuKα radiation at 40KV/40mA at ambient temperature over the Bragg angle (2Theta) range of 5-60 for high-angle and with range of 0-5 for low-angle the crystalline phases were matching by comparing the XRD diffraction patterns of catalysts with reported in the literature. The morphology of mesostructuring can be shown by a transmission electron microscopy (TEM, PHILIPS XL30) and the Bruker EDS was used for the determination of compositional elements in zeolites. Physisorption experiments including, the effective surface area of the catalysts; their pore volume and the pore size distribution from NLDFT model were performed using nitrogen adsorption on a Quantachrom Autosorb instrument.

In order to monitor the concentration , acid strength and heterogeneity of both Brønsted and Lewis acid sites independently,10 mg of zeolite disc was prepared by compacting a certain amount of material in a metallurgical die under 1 bar and admitted to 10% of the in situ infrared energy on a Nicolet iS10 FTIR spectrometer from Thermo scientific in the range 6000-1000 cm^{-1} (resolution 4cm^{-1}) under high vacuum of 10-5 to 10-6 mbar , the disc was activated in vacuum at 30-450°C (ramp 1°C/min.) for 5 hours.IR spectra were recorded in the scale 4000-640 cm^{-1} at different range of temperature and equilibrium pressure. For the quantification of the zeolite acidic properties using FTIR spectra of adsorbed pyridine, the following values of the molar absorption coefficients were applied: ε(B, MFI)=1.08, ε(B, BEA)=1.16, ε(B, MOR)=1.34 and ε(B, FAU)=1.65 cm μmol^{-1} for Brønsted acid sites (BAS, IR peak at ~1545

cm^{-1}) and $\varepsilon(L)$=1.71 cm μmol^{-1} for Lewis acid sites (LAS, IR peak at ~1455 cm^{-1}). The error margin for the acid site quantification was estimated as ±5%. [44] .To gain deeper insight into structural properties of zeolites, physic-chemical information of zeolites used in this work is shown in Table (1).

Table (1) Physico-chemical properties of parent zeolites [45].

Zeolite	Si:Al molar ratio	Ring size (Å)	Pore size (Å)	Internal pore space (Å)
FAU	2.5	12MR	7.4×7.4	11.24
BEA	19	12MR	6.6×6.7 5.6×5.6	6.68
MFI	40	10MR	5.1×5.5 5.3×5.6	6.36
MOR	10	12,8MR	6.5×7.0	-

2.3 Catalytic experiments

The esterification reaction of FFA removal with methanol in the presence of various zeolites was carried out in Biotage microwave synthesiser (Biotage Initiator+). A high precision glass vial 10-20 ml was used in order to improve durable and safe reactions at all times with highly wide range to withstand pressures beyond 30 bar. The microwave heating provides significant thermal impacts, which are relative importance for chemical reaction. The reaction was comprised of adding an excess oleic acid (Sigma-Aldrich, 99%) into grapeseed oil (local market) as 10 vol%, and then reacted with methanol (Fisher Scientific, 99.99%) as 1:30-1:50 molar ratio between them at 100°C for different run times, which varied between 10-30 min. under 5-10 wt% as an amount of the catalyst basis on the oil with continuous automated stirring. The percent FFA (as oleic) were obtained according to reported method in ref 46, with oleic acid and without adding of oleic acid. To a liquid fat mixture 5 g, neutralized 25 ml of Absolute ethanol (Fisher Scientific) and phenolphthalein indicator are added. The sample then is titrated with 0.1 mol L^{-1} of potassium hydroxide KOH (Fisher Scientific, 86%). The % FFA was calculated from below equation:

% FFA = [mL of KOH×mol L^{-1} of KOH×282×10^{-3}/ sample mass (g)] ×100   *(1)*

In addition, the fraction of the FFA removed after separating from methanol and glycerol was used in this work to calculate the conversion of FFA from the oil using below equation:

% Conversion = (FFA$_i$-FFA$_s$/FFA$_i$) ×100   (2)

Where FFA$_s$ is the percent free fatty acid after esterification and FFA$_i$ is the same percent in the oil mixture before the reaction.

Fatty acid composition of the oil was obtained by gas chromatography-mass spectrometry (GC-MS) according to official methods ISO 15884 | IDF 182:2002(E) and ISO 15885 | IDF 184:2002 (E), using GC Agilent 7890A with mass detection system 5975C equipped with a capillary column BPX90 SGE (15m×0.25mm×0.25µm). Additionally, the methyl ester content in the organic layer was determined by GC-FID (Agilent 6890) for the transesterfication reaction between the parent oil and methanol according to the standard test method EN-14103.

Consecutive tests were performed by separating the catalysts, rinsed with methanol and dried overnight at 60°C. The catalysts were characterised again by XRD and FTIR. Then, the recycled catalysts were calcined under the same conditions as prior to the initial reaction and utilised again. The same reaction conditions were used in three recycle runs for these catalysts.

3. Results and discussion

(Figure 1) presents the XRD diffraction patterns of conventional and hierarchical zeolites synthesised in this work. XRD analysis revealed that the treated zeolites still maintain significant crystallinity.This suggests that the treatment of zeolites has been improved successfully without any destruction for the zeolite structure, consistent with previous literatures.[37,42,43] The results of low angle XRD patterns (Figure 2), also indicate that the ordered hexagonal pore arrangement of mesostructured zeolites is observed after the treatment.
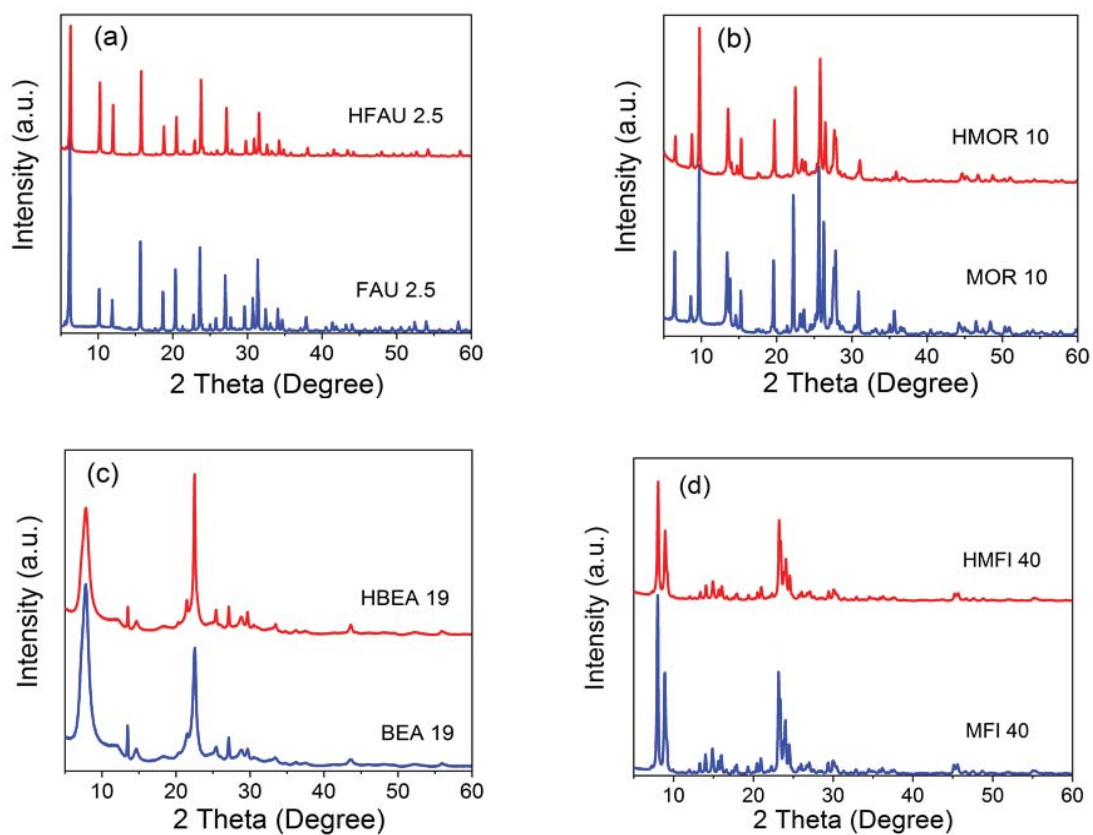
Fig. (1) X-ray diffraction patterns of the zeolites before and after the treatment.
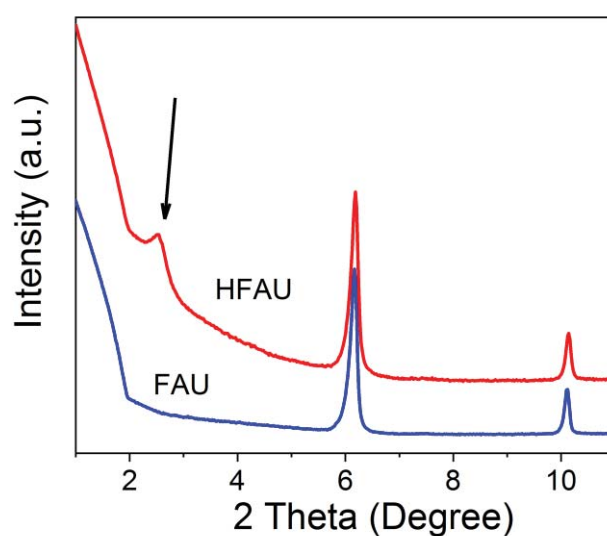

Fig. (2) Low angle XRD patterns of faujasites.

It is relevant to say further evidence in mesoporosity is investigated by the N_2 physisorption isotherms (Figure 3), which shows a type IV isotherm of hysteresis loop for mesoporous materials in this study.[42, 47] In addition; these materials exhibit a significant nitrogen uptake at relative pressure (P/P_o) higher than a pressure in the parent zeolites.
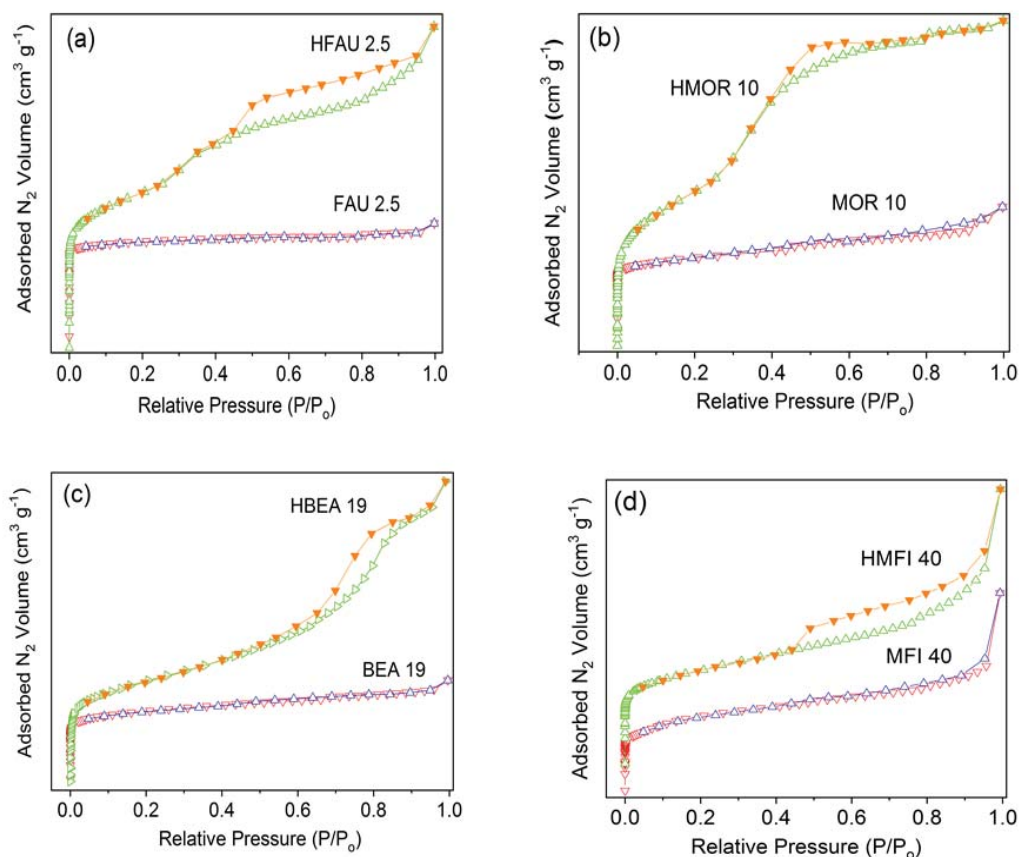

Fig. (3) N_2 adsorption and desorption isotherms for parent and hierarchical zeolites.

In spite of the challenging that associated with surface properties of mesostructured zeolites, some questions regarding the pores and the density of the active site remain answered only inconclusively. These ideas had been put forward earlier in a more extended form by other people in order to explain the mechanism of mesoporsity formation. It should be clearly stated that, and from our previous work, the surfactant templated zeolite mesostructuring strategy was quiet successful for zeolite crystal rearrangement process in one-step by the treating the zeolite with basic solution of surfactant, which led to form mesostructured zeolitic one-phase hybrid material without any an amorphous aluminosilicates (see the images of SEM in Figure 4). In

contrast, the two-steps zeolite recrystallization process usually accompanied with an amorphous phase. [26, 41, 48]
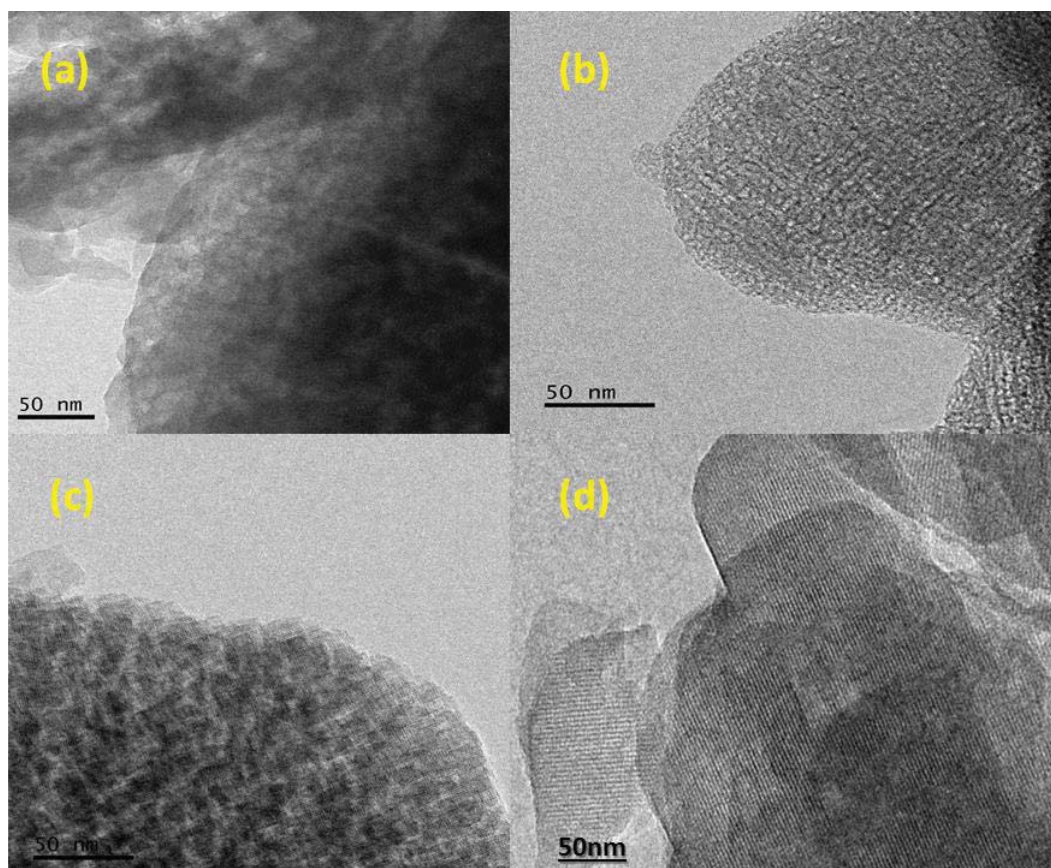

Fig. (4) TEM images for hierarchical (a) FAU, (b) MOR, (c) BEA and (d) MFI.

The textural properties of the mesostructured zeolites depend on the amount of acid or base that utilised in the treatment and the type of surfactant as well as the exposure times. For instance, under the basic media, some of the Si-O-Si bonds are opened, and produce negatively charged sites in the zeolite framework that balance with cationic surfactant. Thus, there is no mesoporosity after the base addition without surfactant, and this combination of surfactant with base is very essential to protect the zeolite structure from possible desilication. This mechanism is working for low aluminium content zeolites such as CP814C (Si:Al = ~19) but not for high aluminium content, for example, the CBV100 cannot undergo the same treatment as in CP814C (Si:Al = ~2.5). This is can be attributed to difficulties of breakage the Si-O-Al bonds under basic medium, and hence, the pre-treatment of acid wash is crucial. The dilute

acid such as citric acid can dealuminate some of the O-Al bonds, which facilities the formation of the mesoporosity in this type of zeolite. However, the surface area and total pore volume both increase with increasing alkaline or acid concentrations in above treatment, while the micropore volume was conserve.[49]

Zeolite acidity including both of frequencies in the Si (OH) Al bands of the Brønsted and Lewis acid sites can be quantified comprehensively by utilising the FTIR spectroscopy. [50] Pyridine is being used in this study in order to calculate the amount and type of acid sites (Table 2) [42].However, it should be noted that ammonia is good candidate for the acid sited in the narrow-pore zeolites with a diameter < 10 Å .[51]

Table (2) Concentration of the acid sites of zeolites based on pyridine adsorption at 150°C.

Zeolite	C_{BAS} , $\mu molg^{-1}$	C_{LAS} , $\mu molg^{-1}$	C_{LAS}/C_{BAS} ratio
FAU2.5	862	48	0.06
HFAU2.5	689	91	0.11
BEA19	409	105	0.26
HBEA19	397	406	1.02
MFI 40	328	29	0.09
HMFI 40	281	57	0.20
MOR10	864	122	0.14
HMOR10	337	149	0.44

Most importantly, all the IR spectroscopy data reported in this work proved that the surface defects formation upon the treatment by surfactant in a basic media is linked with the loss of some of Brønsted acid sites, but increased the Lewis:Brønsted ratio, suggesting formation of hydroxyl nests (silanol terminal group ~ 3740cm^{-1}) see (Figure 5). [42, 52]
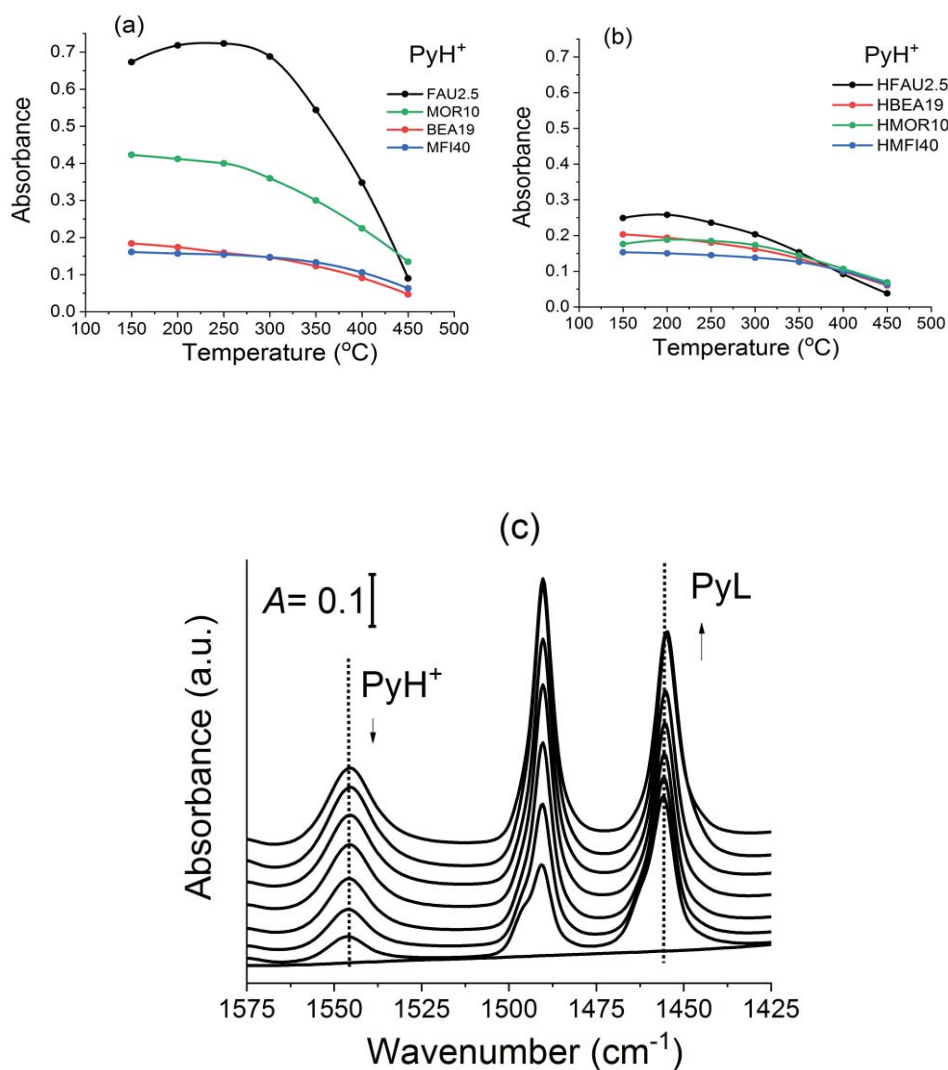
Fig. (5) (a), (b) Pyridine desorption profile with different temperature for parent and hierarchical zeolites; (c) The spectra of pyridine desorption for hierarchical BEA19.

The conversion of oleic acid on various zeolite materials using excess methanol at $100^{\circ}C$ in very shorter time (up to 30 min.) are illustrated in Table (3). It can see from these data, the high conversion appeared on BEA and MFI zeolite catalysts due to a wide pore size and the a robust strength of acid sites for these materials respectively. In accordance with catalytic performance of FAU zeolite in this reaction, although FAU2.5 zeolite has a high amount of acid sites than those of other zeolites, the conversion over this material was not significantly different with

that of MOR10 zeolite. This could be attributed to the amount of acid sites and pore entrance size on MOR10 zeolite, which might also affect to the catalytic reaction. [25, 53] But this is not the whole story; it seems that the introduction of mesoporosity in FAU zeolite induced the high conversion of FFA from oil because of enhancement of acid sites accessibility to oleic acid. Nevertheless, HMOR10 zeolite exhibited similar conversion of FFA compared with parent zeolite despite the diffusion-restricted one-dimensional channel pockets (8-MR) for bulky molecules such as oleic acid.[52,54] The catalytic activity of spent zeolite catalysts did not change significantly after five consecutive runs, confirming that it is possible to recycle these catalysts for several times in esterification reaction.

Table (3) Esterification of grapseed oil over zeolite catalysts.

Run [a]	Catalyst	Conversion [b] (%)	Selectivity (%)
1	FAU2.5	62	>99
1	HFAU2.5	84	>99
1	BEA19	> 95	>99
1	HBEA19	> 95	>99
1	MFI40	> 95	>99
1	HMFI40	> 95	>99
1	MOR10	70	>99
1	HMOR10	73	>99

[a]Reactions were performed in triplicate.
[b]1:40 oil to methanol molar ratio; 30 min reaction time at $100^{o}C$; 7 wt% of catalyst.

The information on the catalytic conditions for the HFAU2.5 zeolite catalyst is presented in (Figure 6). The catalyst amount was adjusted as 7 wt% because there is no change in the conversion after 10 wt%. The reaction time and the molar ratio between oil and methanol can affect the reaction and consolidate it forward. Therefore, we selected three different ratios 1:30, 1:40 and 1:50 with reasonable time range from 10 to 60 minutes under mircrowave heating. Our findings confirmed that the higher molar ratio reduces the mass transfer stage because of the immiscibility between the methanol and oil layers and thus, the rate of esterification increased in a shorter time.
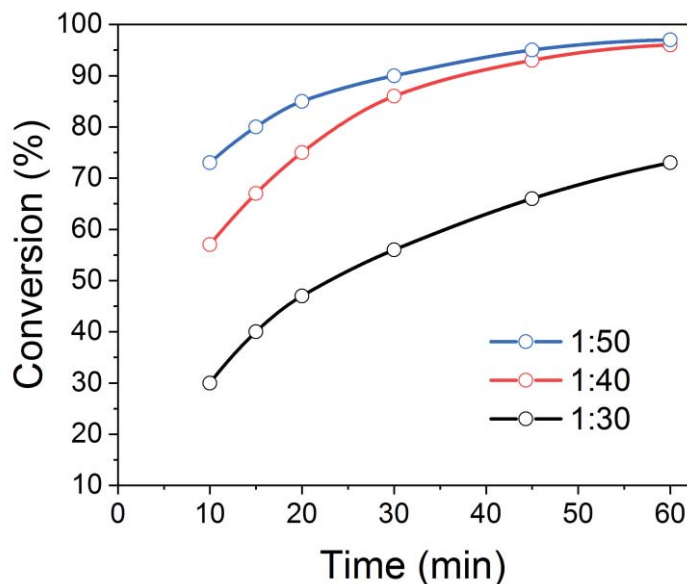
Fig. (6) Effect of the oil to methanol molar ratio on esterification reaction using HFAU2.5 catalyst at different reaction times.

4. Conclusions

Mesostructured zeolites with a binary pore size distribution were prepared in this work using the surfactant-templated strategy and utilised as potential acid catalysts in the esterification reaction of free fatty acid from bio-oil. Although the treatment has not altered the catalytic efficiency of BEA, ZSM-5 and MOR to remove the oleic acid from grapeseed oil, which appears to be determined by the strength of BAS, a higher conversion of oleic acid can be achieved over the hierarchal faujasite zeolite catalyst due to the combination of improved accessibility of stronger acid sites and lower mass transport limitations.. The increase moderate mesoporosity development leads to enhanced the catalytic activity, and give a good opportunity for other zeolite materials such as hierarchical mordenite zeolite catalyst to exploit this material for different zeolite catalysis reactions.

References

1. Perego, C.; Bosetti, A.; Ricci, M.; Millini, R. *Energy Fuels*, **2017**, 31, 7721-7733.

2. Uner, D. *Advances in Refining Catalysis*. : CRC Press; 2017.

3. Armaroli, N.; Balzani, V. *Angew Chem Int Ed*, **2007**, 46, 52-66.

4. Asefa, T.; MacLachlan, M.J.; Coombs, N.; Ozin, G.A. *Nature*, **1999**; 402, 867-871.

5. Vicente, G.; Bautista, L. F.; Rodríguez, R.; Gutiérrez, F.J.; Sádaba, I.; Ruiz- Vázquez, R.M.; Torres-Martínez, S.; Garre, V. *Biochem. Eng. J.*, **2009**, 48, 22-27.

6. Srinivas, D.; Satyarthi, J. K. *Indian J. Chem., Sect. A: Inorg., Bio-inorg., Phys., Theor. Anal. Chem.*, **2012**, 51A, 174-185.

7. Wilson, K.; Lee, A.F. *Catalysis Science & Technology*, **2012**, 2, 884-897.

8. Dhainaut, J.; Dacquin, J-P.; Lee, A.F.; Wilson, K. *Green Chem*, **2010**, 12, 296-303.

9. Ni, J.; Meunier, F.C. *Appl Catal A Gen*, **2007**, 333, 122-130.

10. López, D.E.;Goodwin, J.G. Jr.;Bruce, D.A; Furuta, S. *Appl Catal Gen.*, **2008**, 339,76-83.

11. Mbaraka, I.K.; Radu, D.R.; Lin, V.S.Y.;Shanks, B.H. *J Catal*, **2003**, 219, 329-336.

12. Melero, J.A.; Bautista, L.F.; Morales, G.; Iglesias, J.; Briones, D. *Energy Fuel*, **2008**, 23, 539-547.

13. Garg, S.;Soni, K.; Kumaran, G.M.; Bal, R.; Gora-Marek, K.; Gupta, J.K.; Sharma, L.D.; Dhar, G.M. *Catal Today*, **2009**, 141:125-129.

14. Dacquin, J.P.; Lee, A.F.; Pirez, C.; Wilson, K. *Chem Commun*, **2012**, 48, 212-214.

15. Pirez, C.; Lee, A.F.; Manayil, J.C.; Parlett, C.M.A.; Wilson, K. *Green Chem*, **2014**, 16, 4506-4509.

16. Pirez, C.; Caderon, J-M.; Dacquin, J-P.; Lee, A.F.; Wilson, K. *ACS Catal*, **2012**, 2, 1607-1614.

17. Pirez, C.; Reche, M.T.; Lee, A.F.; Manayil, J.C.; dos-Santos, V.C.; Wilson, K. *Catal Lett*, **2015**, 145, 1483-1490.

18. Alsalme, A.; Kozhevnikova, E.F.; Kozhevnikov, I.V. *Appl Catal Gen*, **2008**, 349:170-176.

19. Leng, Y.; Wang, J.; Zhu, D.; Wu, Y.; Zhao, P. *J Mol Catal A Chem.*, **2009**, 313, 1-6.

20. Dufaud, V.; Lefebvre, F.; Niccolai, G.P.; Aouine, M. *J Mater Chem.*, **2009**, 19, 1142-1150.

21. Narasimharao, K.; Brown, D.R.; Lee, A.F.; Newman, A.D.; Siril, P.F.; Tavener, S.J.; Wilson, K. *J Catal*, **2007**, 248, 226-234.

22. Pesaresi, L.; Brown, D.R.; Lee, A.F.; Montero, J.M.; Williams, H.; Wilson, K. *Appl Catal A Gen.*, **2009**, 360, 50-58.

23. López, D.E.; Suwannakarn, K.; Bruce, D.A.; Goodwin, J.G. Jr. *J Catal*, **2007**, 247, 43-50.

24. Chung, K.; Chang, D.; Park, B. *Bioresour Technol*, **2008**, 99, 7438-7443.

25. Chung, K.; Park, B. *J. Ind. Eng. Chem*, **2009**;15, 388-392.

26. Davis, M.E. *Mesoporous zeolites: preparation, characterization and Applications.* John Wiley & Sons; 2015.

27. Verboekend, D.; Pérez-Ramírez, J. *Catalysis Science & Technology*, **2011**; 1, 879-890.

28. Silaghi, M.; Chizallet, C.; Raybaud, P. *Microporous Mesoporous Mater*, **2014**; 191, 82-96.

29. Milina, M.; Mitchell, S.; Michels, N-L.; Kenvin, J.; Pérez-Ramírez, J. *J Catal*, **2013**, 308, 398-407.

30. Huang, S.; Liu, X.;Yu, L.; Miao, S.; Liu, Z.; Zhang, S.; Xie, S.; Xu, L.*Microporous Mesoporous Mater*, **2014**, 191, 18-26.

31. Serrano, D.P.; Sanz, R.; Pizarro, P.; Moreno, I.;Shami, S. *Microporous Mesoporous Mater*, **2014**, 189, 71-82.

32. Jiang, J.; Yu, J.; Corma, A. *Angew Chem Int Ed*, **2010**, 49, 3120-3145.

33. Perez-Ramirez, J.;Christensen, C.H.;Egeblad, K.;Christensen, C.H.;Groen, J.C. *Chem Soc Rev*, **2008**, 37, 2530-2542.

34. Čimek, A.; Subotić, B.; Šmit, I.; Tonejc, A.; Aiello, R.;Crea, F.; Nastro, A. *Microporous Materials*, **1997**, 8, 159-169.

35. Mitchell, S.; Pinar, A.B.; Kenvin, J.; Crivelli, P.; Kärger, J.; Pérez-Ramírez, J. *Nat Commun*, **2015**, 6, 8633.

36. Opanasenko, M.V.; Roth, W.J.; Cejka, J. *Catalysis Science & Technology*, **2016**, 6, 2467-2484.

37. García-Martínez, J.; Johnson, M.; Valla, J.;Li, K.; Ying, J.Y. *Catalysis Science & Technology*, **2012**; 2, 987-994.

38. Sachse, A.; Garcia-Martinez, J. *Chemistry of Materials*, **2017**, 29, 3827-3853.

39. Milina, M.; Mitchell, S.; Pérez-Ramírez, J. *Catal Today*, **2014**; 235, 176-183.

40. Osatiashtiani, A.; Puértolas, B.; Oliveira, C.C.;Manayil, J.C.; Barbero, B.; Isaacs, M., Michailof, C.; Heracleous, E.; Pérez-Ramírez, J.; Lee, A.F. *Biomass Conv. Bioref.*, **2017**, 7, 331-342.

41. Al-Ani, A.; Darton, R.; Sneddon, S.; Zholobenko, V. *ACS Applied Nano Materials*, **2018**, 1, 310-318.

42. Al-Ani, A.; Haslam. J.C.J.; Mordvinov. N. E. ; Lebedev O. I.; A. Vicente, Fernandez C., Zholobenko. V. Zeolites. *RSC Nanoscale Advances*, **2019**, 1, 2029-2039.

43. Pérez-Ramírez, J.; Verboekend, D.; Bonilla, A.; Abelló, S. *Adv Func Mater*, **2009**, 19, 3972-3979.

44. Emeis C. *J. Catal.,* **1993**, 141, 347-354.

45. Jae, J., Tompsett, G.A.; Foster, A.J.; Hammond, K.D.; Auerbach, S.M.; Lobo, R.F., Huber, G. W. *J. Catal.,* **2011**, 279, 257-268.

46. O'Keefe, S.F.;Pike, O.A. *Fat characterization. Food analysis*: Springer; 2010, p. 239-260.

47. Cychosz, K.A.; Guillet-Nicolas, R., García-Martínez, J., Thommes, M. *Chem Soc Rev*., **2017**, 46, 389-414.

48. Prasomsri, T.; Jiao, W.; Weng, S.Z.; Martinez, J.G. *Chem. Comm.*, **2015,** 51, 8900-8911.

49. Sachse, A.; Grau-Atienza, A.; Jardim, E.O.; Linares, N.; Thommes, M.; Garcia-Martinez, J. *Crys. Growth. Des*., **2017**, 17, 4289-4305.

50. Datka, J.; Kawałek, M.; Góra-Marek, K. *Appl. Catal. Gen.*, **2003**, 243, 293-299.

51. Datka, J.; Góra-Marek, K. *Catal Today*, **2006**, 114, 205-210.

52. Datka, J.;Tarach,K.; Góra-Marek, K. *Acidic properties of hierarchical zeolites. Mesoporous Zeolites: Preparation, Characterization and Applications*. John Wiley & Sons; 2015, p.461-496.

53. Milina, M.; Mitchell, S.; Michels, N.; Kenvin, J.; Pérez-Ramírez, J. *J. catal*., **2013**, 308, 398-407.

54. Pastvova, J.; Kaucky, D.; Moravkova, J.; Rathousky, J.; Sklenak, S.; Vorokhta, M.; Brabec, L.; Pilar, R.; Jakubec, I.; Tabor, E. *ACS Catal.*, **2017**, 7, 5781-5795.